Appendix F. Determining earthquake recurrence rates

For each earthquake, a set of source parameters must be chosen that determines the initial condition for propagation modeling. Earthquake magnitude is the primary parameter that links other source parameters such as rupture area and average amount of slip. Unlike deterministic modeling in which recurrence rates are not considered, probabilistic modeling requires the determination of recurrence rate for each source used in inundation modeling. Recurrence rates can be determined from frequency-magnitude distributions as follows.

F1. Characteristic vs. Gutenberg-Richter

A persistent controversy in seismology is whether the frequency-magnitude distribution for earthquakes follows a characteristic model at the largest magnitudes or a modified Gutenberg-Richter (G-R) distribution. Although broad generalizations are not always accurate, observational seismology tends to support the modified G-R model, whereas paleoseismology studies tend to follow, at least implicitly, the characteristic model. Figure F-1a, modified from Wesnousky (1994), shows the two models for both the discrete and cumulative form, where M_a is the magnitude of the largest aftershock for the characteristic distribution. Note that for both models, smaller earthquakes follow a power-law scaling relationship. In Wesnousky's (1994) conception that is typical for paleoseismic studies, there is a significant gap in intermediate earthquake magnitudes between M_a and M_{max} for the characteristic model such that a given fault typically ruptures in M_{max} earthquakes with the rest of the distribution $M < M_a$ representing foreshocks, aftershocks, and background seismicity. In contrast, the G-R model predicts a power-law scaling relationship that is valid for all magnitudes up to M_{max}.

Both models are often employed in the development of the USGS National Seismic Hazard Maps. For example, in the seismic hazard maps for Alaska (Wesson *et al.*, 1999) the Aleutian segment of the Pacific-North American interplate thrust is characterized by a G-R distribution for M = 7–9.2, whereas the Prince William Sound segment (1964 source region) is characterized by both a G-R distribution (M = 7–8) and a characteristic rupture model (M = 9.2) with an average return time of 750 years derived from paleoseismology studies (400–500 years estimated by Bartsch-Winkler and Schmoll, 1992). For earthquakes along the Cascadia interplate thrust, the National Seismic Hazard Maps use two different models that are equally weighted (Frankel *et al.*, 2002): (1) a M = 9.0 characteristic earthquake with an average repeat time of 500 years

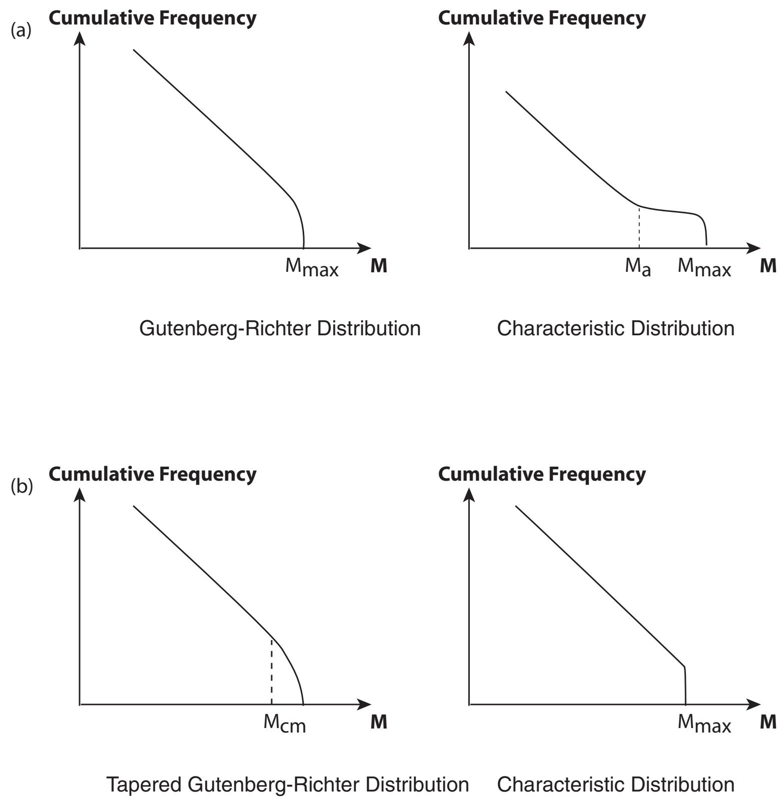

Figure F1: Characteristic and Gutenberg-Richter earthquake distributions as described in different studies: (a) Wesnousky (1994); (b) Kagan (2002a).

and (2) a series of M = 8.3 earthquakes that fill the seismogenic region of the interplate thrust every 500 years, resulting in a repeat time of 110 years for a M = 8.3 earthquake to occur anywhere in the seismic zone. A G-R distribution is not used for Cascadia interplate thrust earthquakes. It should be stressed, however, that the paleoseismic data used in characteristic earthquake models needs to be carefully analyzed with respect to the possible magnitude range that geologic markers represent and to account for open intervals in calculating average repeat times (Parsons, 2004, submitted) (see also Savage, 1991; Schwartz, 1999 for specific concerns regarding the characteristic model).

A different definition of characteristic and Gutenberg-Richter models is presented more recently by Kagan (2002a) as shown in Fig. F1b. The characteristic distribution is a power-law distribution truncated at the characteristic magnitude (cumulative form). This is similar to Wesnousky's (1994) definition of Gutenberg-Richter distribution (Fig. F1a) and hence is an obvious source of confusion. The other distributions shown above are modified Gutenberg-Richter distributions where there is an accelerating fall-off in earthquake recurrence rates with increasing magnitude. The tapered Gutenberg Richter and Gamma distributions have a "soft" corner magnitude, whereas the characteristic and truncated Pareto (also called truncated Gutenberg-Richter because the probability density distribution is truncated) have "hard" cutoff magnitudes (Kagan, 2002b).

For tsunamis, we are primarily concerned with establishing recurrence rates for large magnitude earthquakes that occur at the tail of these distributions. The distributions derived by Kagan are statistically more defensible using observed seismicity and seismic moment balances (Bird and Kagan, submitted; Kagan, 2002a; Pisarenko and Sornette, 2004; Sornette and Sornette, 1999). Even so, there is substantial uncertainty in establishing recurrence rates at the distribution tails because of a lack (thankfully) of very large magnitude earthquakes (hence, the reason there are multiple distributions).

F2. Modified G-R Distributions

The original form of the G-R distribution is

$$\log N(m) = a - bm, \tag{F1}$$

where $N(m)$ is the number of earthquakes with magnitude $\geq m$ and a and b are scaling parameters. The parameter a is often associated with the seismic activity of a particular region and b is the power-law exponent of scaling. Kagan (2002a), Sornette and Sornette (1999), and other earlier studies indicate that source finiteness requires that there must be an upper bound to the G-R distribution (Equation 1). This leads to the modified G-R distributions described by Kagan (2002a) and shown in Fig. F1b.

In a simplified version involving the truncated G-R distribution, Ward (1994) derives an expression for the average repeat time for earthquakes of magnitude m:

$$T(m) = \left[\frac{b}{1.5+b}\right] \frac{10^{(1.5+b)m_{\max}+9.5}}{\dot{M}_s\left[10^{bm_{\max}} - 10^{bm}\right]}, \tag{F2}$$

where $\dot{M}_s$ is the seismic moment release rate in Nm/yr. Note that the a-value (Equation 1) does not appear in this expression. The seismic activity is determined by $\dot{M}_s$ as described below. Recurrence rates calculated from (2) are associated with a sharp distribution corner with a hard cutoff at $m_{\max}$.

An equivalent expression for the tapered G-R (TGR) distribution can be derived from Kagan (2002b, eqn. 7):

$$T(M_0) = \left[\frac{1}{1-\beta}\right] \frac{M_0^{\beta} M_{\mathrm{cm}}^{1-\beta}}{\dot{M}_s} \Gamma(2-\beta)\xi_m, \tag{F3}$$

where $\beta = \frac{2}{3}b, \Gamma$ is the gamma function and $\xi_m = \exp(M_0/M_{\mathrm{cm}})$. M_0 and M_{cm} are given in Nm (corresponding magnitudes m_0 and m_{cm} are given by $m = \frac{2}{3}\log M - 6.0$). Similar expressions can be derived for the other distributions.

F3. Seismic Moment Conservation

The seismic moment rate $\dot{M}_s$ in Equations (2) and (3) can be determined for a particular seismic zone from historic earthquakes, as long as the catalog contains the largest seismic moment events. Otherwise, $\dot{M}_s$ can be determined from fault slip rates ($\dot{s}_{\text{geol}}$) and estimates of geometric parameters. The formula for geologically determined $\dot{M}_s$ is given below (Ward, 1994):

$$\dot{M}_s = \mu L H_s \dot{s}_{\text{geol}} \tag{F4}$$

where μ is the shear modulus, L is the fault length, and H_s is the effective seismogenic thickness. The latter parameter is the most difficult to estimate because it involves determination of the base of seismicity (transition from unstable to stable frictional properties) and the seismic coupling coefficient (χ) that accounts for the portion of fault movement that occurs aseismically. Studies by Bird and Kagan (submitted), Kagan (2002b), and Ward (1994) all seek to ensure that the seismic moment rates are consistent with plate tectonic rates and physical parameters.

F4. Seismic Zonation

In calculating frequency-magnitude distributions, a seismic zonation scheme is used such that the scaling parameters can be considered more or less uniform. For example, the zonation scheme used by Ward (1994) for evaluating onshore seismic hazards in southern California entailed defining 66 regions with definable characteristics. For the purpose of the tsunami pilot study, much larger zones need to be considered. For far-field sources, the Flinn-Engdahl regions are probably most suitable. Kagan (1997) and Sornette and Sornette (1999) determine b-values, moment rate, and corner magnitudes for Flinn-Engdahl regions relevant to far-field tsunamis. In a later paper, Kagan (2002b) considers smaller circum-Pacific seismic zones defined by McCann *et al*. (1979) and Nishenko (1991). For the smaller zones, however, the statistics are not as reliable and accommodation for interacting zones (cf., Ward, 1994) needs to be included for larger earthquakes that span multiple zones.

A question may be raised as to whether the estimated scaling parameters are applicable for the subset of tsunamigenic earthquakes. The earthquakes analyzed by Kagan (1997; 2002b) are in the depth range of 0–70 km, though most are in the 0–40 km range. The primary condition that limits the transfer of seismic to tsunami energy is deformation that occurs onshore rather than offshore. This effect should be accounted for in existing tsunami propagation models that use realistic bathymetry and topography over the source region.

F5. Approach Used in This Study

As outlined above, there are several choices of frequency-magnitude distributions that one could choose to determine earthquake recurrence rates. Whereas the scaling and recurrence rates of small earthquakes are usually well defined, the tail of the distribution is difficult to constrain with statistical confidence (Pisarenko and Sornette, 2004). Unfortunately, it is the large earthquakes that exist at the distribution tail that are of primary interest for far-field tsunami studies.

One possible approach is to calculate inundation maps based on M_{max}, some of which have historic precedent, such as the 1964 Alaska, 1960 Chile, 1957 Aleutian, and 1700 Cascadia earthquakes. This serves the dual purpose of constraining the aggregate 0.01 or 0.002 annual probability from high return-period events and using these historic events for model validation. However, how do we establish the return period for these events? Sykes and Quittmeyer (1981) use the time-predictable model (Shimazaki and Nakata, 1980) to estimate recurrence rates for large earthquakes in most of the regions of interest. Murray and Segall (2002), however, recently call into question the time-predictable model. As another option, we can use characteristic rates for the 1964 Alaska source and 1700 Cascadia source regions (similar to the National Seismic Hazard Maps) estimated from paleoseismology and use a modified G-R distribution for other regions defined by Flinn-Engdahl zonation. If characteristic sources are used, however, it would be most consistent to also use historic and paleoseismic studies for other regions, such as Japan, that are considerably more complex (e.g., Nanayama *et al.*, 2003; Rikitake, 1999; Utsu, 1984). This also introduces the previously mentioned problems in using paleoseismic data to establish recurrence rates for specific earthquake magnitudes. A third approach would be to simply use a modified G-R distribution for all regions that are constrained by plate tectonic/fault slip rates. In this case, the seismic moment rate for the Cascadia interplate thrust would have to be derived from fault slip rates (Equation 4) and an assumed b-value. In contrast to the paleoseismic/characteristic earthquake approach, both the magnitude and recurrence rates are well defined, though there is significant uncertainty in estimating recurrence rates for the largest earthquakes.

F6. Summary

One of the obvious difficulties with specifying far-field sources for this and any tsunami probability study is obtaining accurate estimates for M_{max} and the associated recurrence rates for each source region. Several problematic examples include wide variations in the estimated seismic moment for the 1957 Andreanof earthquake (Boyd *et al.*, 1995) and differences between tsunami and seismic estimates for events such as the 1952 Kamchatka and 1960 Chile earthquakes. One way to incorporate these uncertainties is to estimate a reasonable distribution of source parameters and run additional models to determine the effect on inundation at Seaside. Given the time constraint of the pilot study, however, we rely on sensitivity studies such as Titov *et al.* (1999) to determine if and how this type of analysis should proceed.

Finally, an example of how these sources may combine for determining the 100-year and 500-year inundation zones is given below. If we assume a time-independent (Poissonian) probability model and that the largest inundation zone will be from a M = 9 Cascadia earthquake with an average return time of 500 years, then the Cascadia earthquake alone (along with its variations) will determine the 500-year tsunami flood at Seaside. Suppose, furthermore, that the four largest inundation zones at Seaside were from a M = 9.0 Cascadia event (500 yr), a M = 9.2 Gulf of Alaska event (750 yr), a M = 8.8 Kamchatka event (300 yr), and a M = 9.5 Chile event (300 yr) Then, the 100-year tsunami flood would be where the inundation zones from all four of these earthquakes overlap (i.e., $\frac{1}{500}+\frac{1}{750}+\frac{1}{300}+\frac{1}{300}=\frac{1}{100}$). These numbers are approximate for the purposes of the example. Also, the combination of events constraining the 100-year flood may change when time-dependent probabilities are considered.

F7. References

Bartsch-Winkler, S., and H.R. Schmoll, 1992, Utility of radiocarbon-dated stratigraphy in determining late Holocene earthquake recurrence intervals, upper Cook Inlet region, Alaska. *Geological Society of America Bulletin, 104*, 684–694.

Bird, P., and Y.Y. Kagan, submitted, Plate-tectonic analysis of shallow seismicity: Apparent boundary width, beta-value, corner magnitude, coupled lithosphere thickness, and coupling in seven tectonic settings. *Bulletin of the Seismological Society of America*.

Boyd, T.M., E.R. Engdahl, and W. Spence, 1995, Seismic cycles along the Aleutian arc: Analysis of seismicity from 1957 through 1991. *Journal of Geophysical Research, 100*, 621–644.

Frankel, A.D., M.D. Petersen, C.S. Mueller, K.M. Haller, R.L. Wheeler, E.V. Leyendecker, R.L. Wesson, S.C. Harmsen, C.H. Cramer, D.M. Perkins, and K.S. Rukstales, 2002, Documentation for the 2002 Update of the National Seismic Hazard Maps. U.S. Geological Survey, Open-File Report 02-420, 33 pp.

Kagan, Y.Y., 1997, Seismic moment-frequency relation for shallow earthquakes: Regional comparison. *Journal of Geophysical Research, 102*, 2835–2852.

Kagan, Y.Y., 2002a, Seismic moment distribution revisited: I. Statistical Results. *Geophysical Journal International, 148*, 520–541.

Kagan, Y.Y., 2002b, Seismic moment distribution revisited: II. Moment conservation principle. *Geophysical Journal International, 149*, 731–754.

McCann, W.R., S.P. Nishenko, L.R. Sykes, and J. Krause, 1979, Seismic gaps and plate tectonics: Seismic potential for major boundaries. *Pure and Applied Geophysics, 117*, 1082–1147.

Murray, J., and P. Segall, 2002, Testing time-predictable earthquake recurrence by direct measurement of strain accumulation and release. *Nature, 419*, 287–291.

Nanayama, F., K. Satake, R. Furukawa, K. Shimokawa, B.F. Atwater, K. Shigeno, and S. Yamaki, 2003, Unusually large earthquakes inferred from tsunami deposits along the Kuril trench. *Nature, 424*, 660–663.

Nishenko, S.P., 1991, Circum-Pacific seismic potential: 1989–1999. *Pure and Applied Geophysics, 135*, 169–259.

Parsons, T., 2004, Recalculated probability of M 7 earthquakes beneath the Sea of Marmara, Turkey. *Journal of Geophysical Research, 109*(B5), B05304, doi: 10.1029/2003JB002667.

Parsons, T., submitted, Significance of stress transfer in time-dependent earthquake probability calculations.

Pisarenko, V.F., and D. Sornette, 2004, Statistical detection and characterization of a deviation from the Gutenberg-Richter distribution above magnitude 8. *Pure and Applied Geophysics, 161*, 839–864.

Rikitake, T., 1999, Probability of a great earthquake to recur in the Tokai district, Japan: Reevaluation based on newly-developed paleoseismology, plate tectonics, tsunami study, micro-seismicity and geodetic measurements. *Earth Planets Space, 51*, 147–157.

Savage, J.C., 1991, Criticism of some forecasts of the National Earthquake Prediction Evaluation Council. *Bulletin of the Seismological Society of America, 81*, 862–881.

Schwartz, S.Y., 1999, Noncharacteristic behavior and complex recurrence of large subduction zone earthquakes. *Journal of Geophysical Research, 104*, 23,111–23,125.

Shimazaki, K., and T. Nakata, 1980, Time-predictable recurrence model for large earthquakes. *Geophysical Research Letters, 7*, 279–282.

Sornette, D., and A. Sornette, 1999, General theory of the modified Gutenberg-Richter law for large seismic moments. *Bulletin of the Seismological Society of America, 89*, 1121–1130.

Sykes, L.R., and R.C. Quittmeyer, 1981, Repeat times of great earthquakes along simple plate boundaries. In *Earthquake Prediction: An International Review*, Simpson, D.W., and P.G. Richards (eds.), Washington, D.C., American Geophysical Union, 217–247.

Titov, V.V., H.O. Mofjeld, F.I. González, and J.C. Newman, 1999, Offshore forecasting of Hawaiian tsunamis generated in Alaskan-Aleutian subduction zone. Pacific Marine Environmental Laboratory (PMEL), NOAA Technical Memorandum ERL PMEL-114, 26 pp.

Utsu, T., 1984, Estimation of parameters for recurrence models of earthquakes. *Bulletin of the Earthquake Research Institute, 59*, 53–66.

Ward, S.N., 1994, A multidisciplinary approach to seismic hazard in southern California. *Bulletin of the Seismological Society of America, 84*, 1293–1309.

Wesnousky, S.G., 1994, The Gutenberg-Richter or characteristic earthquake distribution, which is it? *Bulletin of the Seismological Society of America, 84*, 1940–1959.

Wesson, R.L., A.D. Frankel, C.S. Mueller, and S.C. Harmsen, 1999, Probabilistic Seismic Hazard Maps of Alaska. U.S. Geological Survey, Open-File Report 99-36, 20 pp.